Lateral distribution of muon pairs in underground cosmic ray showers

1970 J. Phys. A: Gen. Phys. 3 689

(http://iopscience.iop.org/0022-3689/3/6/009)

J. Phys. A: Gen. Phys., 1970, Vol. 3. Printed in Great Britain

Lateral distribution of muon pairs in underground cosmic-ray showers†

R. B. COATS,‡ S. OZAKI,§ R. O. STENERSON,
H. E. BERGESON, J. W. KEUFFEL, M. O. LARSEN,
G. H. LOWE, J. L. OSBORNE‡ and J. H. PARKER
Department of Physics, University of Utah, Salt Lake City, Utah, U.S.A.
MS. received 6th May 1970

Abstract. The lateral distribution of cosmic-ray muon showers underground has been studied by measuring the separations between about 5000 pairs of muons. Results are presented in terms of a counting rate for an equivalent pair of one metre-square detectors beneath 2500 hg cm^{-2} rock and orientated at 45° zenith. For separations from 0 to 50 m an approximately exponential dependence of the counting rate on detector separation is observed which decreases by a factor e in of the order of 10 m.

1. Introduction

Underground muon showers, which are a prominent feature of observations with the University of Utah neutrino detector, offer a unique opportunity to study interactions of cosmic-ray primaries having energies of hundreds of TeV. This paper describes the results of a study made during the first six months of running with the completed Utah detector. The emphasis of this work is on the measurement of the radial distribution of muons in showers, which provides an experimental basis for inferring the transverse momentum distribution of the secondary particles produced by a primary cosmic ray. The related study of shower multiplicity distributions will be discussed in future papers. An analysis of the present data, using a conservative interaction model, is given in the immediately following paper by Adcock *et al.* (1970—to be referred to as II).

2. Data gathering

The Utah detector has been described in detail elsewhere (Keuffel and Parker 1967, Hilton *et al.* 1967 and Bergeson *et al.* 1967) so only the features of the detector pertinent to this paper will be described. Muon showers are detected by means of four large water Čerenkov counters, and the trajectories of the individual muons are determined by 600 cylindrical spark counters (CSC's) mounted in 15 vertical columns about the Čerenkov counters (figure 1). Typically, the track of a muon can be located with a spatial accuracy of a few centimetres, resulting in an angular resolution of the order of 1°. The dimensions of the detector are such that the maximum distance between muons traversing it is of the order of 10 m.

In addition to the main detector, three outrigger detectors (α, β and γ in figure 2) mounted on movable mine cars are located in an adjacent tunnel. Each outrigger consists of 24 CSC's mounted in 3 horizontal planes, with 8 CSC's per plane. The main detector provides the trigger for the outriggers, which then record muons associated with the shower in the main detector. Initially the outriggers were located in

† Supported by the National Science Foundation (U.S.A.)
‡ Present address: University of Durham, Durham, England.
§ Present address: Osaka City University, Osaka, Japan.

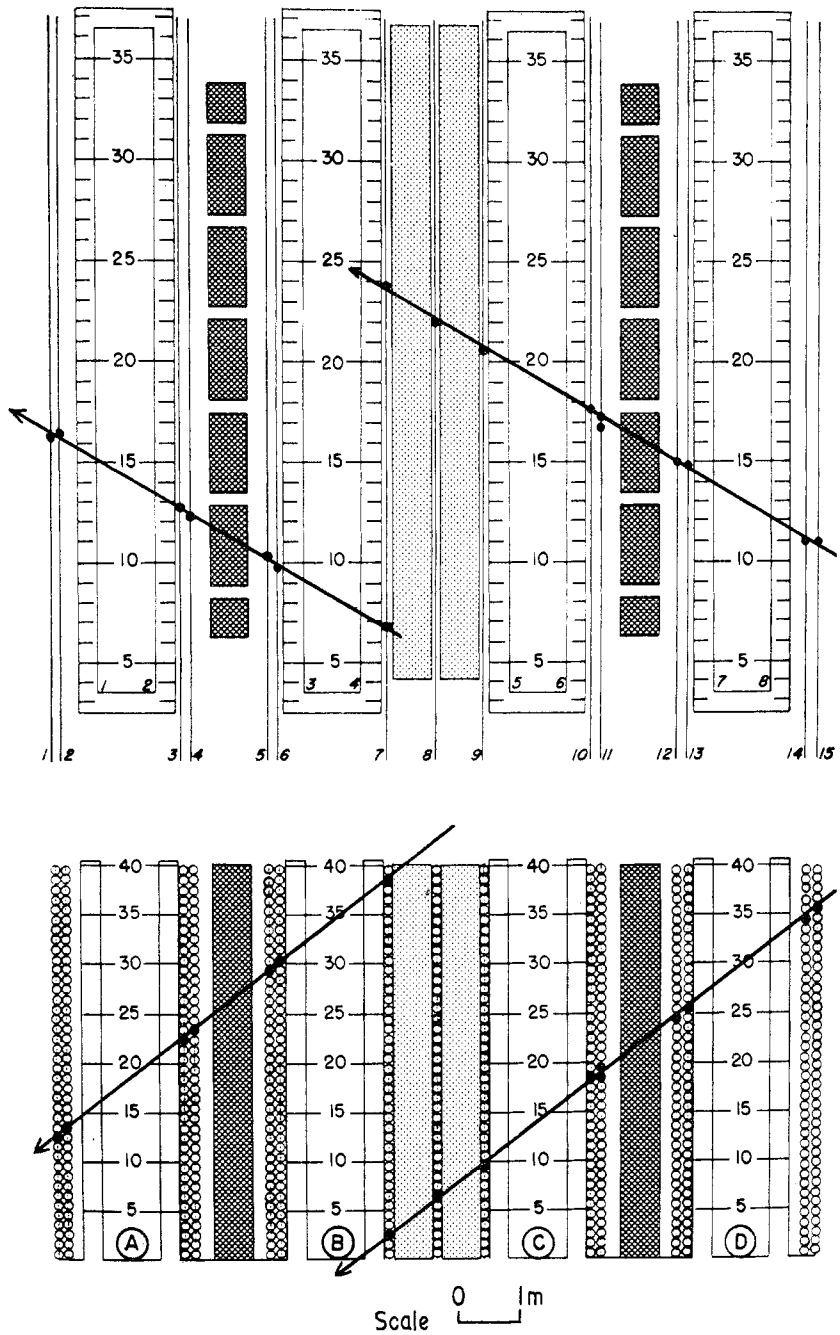

Figure 1. Front (XZ plane) and top (XY plane) views of the University of Utah detector. In the front view, cylindrical spark counters are seen end-on as circles stacked in columns 40 high on either side of water-filled Čerenkov tanks labelled A, B, C, D. The dark cross-hatched areas between A and B and between C and D are the solid iron magnets. The light dotted areas between B and C are concrete blocks. In the top view, columns of sonic cylindrical spark counters appear as lines labelled 1 to 15, and the light-collecting walls of the Čerenkov tanks are labelled 1 to 8. The 8 groups of spark chambers are the columns that follow: 1 and 2, 3 and 4, 5 and 6, 7, 9, 10 and 11, 12 and 13, and 14 and 15.

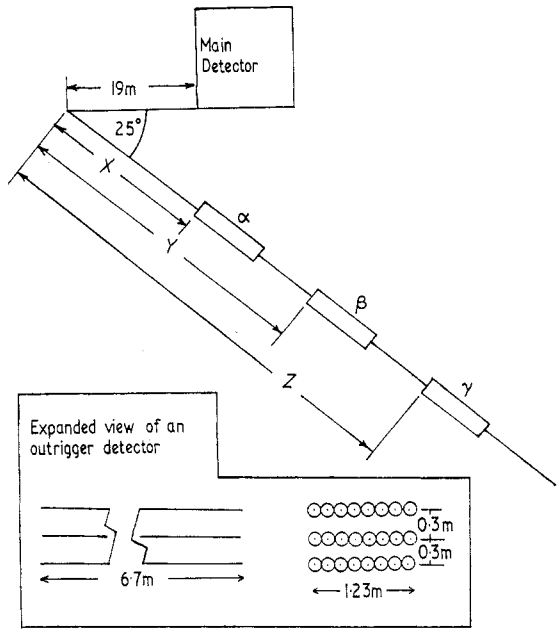

Figure 2. The movable outrigger detectors α, β and γ are shown in the plan view above together with the main detector. Each outrigger detector is comprised of 3 planes of 8 sonic cylindrical spark counters (see inset). In Position 1, X = 24·9m, Y = 37·1m, Z = 49·3m. In Position 2, X = 24·9m, Y = 57·9m, Z = 84·6m.

Position 1 (figure 2), for which the maximum separation between a pair of muons was approximately 45 m. Later β and γ were moved to Position 2 (figure 2), so increasing the maximum detectable separation between a pair of muons to approximately 80 m. Owing to the CSC planes in an outrigger detector being more closely spaced than the planes in the main detector, the angular resolution of the outrigger is only about 10°. However, the following stringent criteria are imposed on the selection of events to ensure that the tracks detected in the outriggers are associated with the main detector event.

(i) The track in an outrigger must be parallel to the track(s) in the main detector to within the resolution of each detector.

(ii) Only those tracks in an outrigger which have three co-linear sparks, one in each plane of CSC's, are accepted. This results in a 10% loss of events due to CSC inefficiencies, for which a correction is made.

(iii) All CSC pipes are sensitive for only 2 μs after the main detector has triggered. This reduces the rate of unassociated muons in the outriggers to negligible proportions.

As a measure of the spurious background the outriggers were pulsed at random for the equivalent of 100 days running time, the length of time over which the data presented in this paper were recorded, and no track was observed which could have satisfied even criterion (ii) above. Therefore it can be definitely concluded that the tracks observed in the outriggers were produced by muons associated with the muons triggering the main detector.

During the period from January to June 1969, 5507 pairs of muons with separations greater than 1 m, incident at zenith angles ranging from 40 to 70° and having traversed a thickness of rock in the range 1900 to 4000 hg cm^{-2}, were recorded and analysed.

3. Analysis

3.1. *Introduction*

The complexity of the aperture and triggering requirements of the Utah detector make it desirable to present the data in a manner that is independent of detector geometry. The technique adopted, which has been described previously by Porter and Stenerson (1969), is to display the data in the form of a decoherence curve, which is defined as the counting rate per second per steradian of a pair of 1 m^2 detectors operated in coincidence, as a function of their separation. The following sections describe the analysis of the data.

3.2. *The main detector*

The main detector is triggered when a coincidence is formed between two or more of the Čerenkov counters, and this condition must be taken into consideration when evaluating the number of equivalent 1 m^2 detectors. Essentially, the area presented to a muon shower incident within a $2\frac{1}{2}°$ zenith (θ) $\times$ 5° azimuth (ϕ) bin is divided into 1 m^2 areas such that a muon incident on any one area would traverse at least three spark counter groups (figure 1). Pairs of areas are then selected which satisfy the Čerenkov triggering condition of at least two tanks struck within prescribed limits. The separation x between each pair is calculated, and the pairs are sorted into separation bins of width 1 m in the range 0 to 10 m. In this way the number of equivalent pairs of 1 m^2 detectors with separation x is determined for any bin. In practice the total area is divided into areas smaller than 1 m^2, so as to reduce edge effects and bin-size effects in the calculation. Associated with each θ–ϕ bin is a depth of rock h, so at this stage conversion is made from θ–ϕ bins to θ–h bins, and the calculated numbers of pairs of 1 m^2 detectors are regrouped with respect to h.

The data are analysed in the following way. Suppose a shower of muons strikes the main detector. Pairs of muons are selected such that each muon satisfies the spark counter group requirement and which, taken *together*, could have triggered the detector. The event efficiency is determined from the measured Čerenkov efficiencies (Bergeson *et al.* 1967, Keuffel *et al.* 1970), taking into account *all* muons in the event. The separation between the muons in an accepted pair is calculated, and pairs are than sorted into bins according to x, θ and h, with the appropriate correction being made for efficiency. Division by the number of equivalent pairs of 1 m^2 detectors as calculated above results in decoherence curves for various h and θ ranges.

3.3. *Outriggers*

The outrigger analysis is basically the same as for the main detector. The one major difference arises from the fact that the outrigger trigger is provided by the main detector, and concerns the acceptance area of the main detector. Since pairs of muons contributing to the outrigger decoherence curve comprise one muon through an outrigger and one through the main detector, then only those shower muons traversing the main detector which *individually* satisfy the triggering criteria can be considered. The procedure for obtaining decoherence curves is the same as described in § 3.2, event efficiencies again being determined taking into account *all* muons in the main detector, and the inefficiency of the outriggers.

3.4. *Combination of data*

More underground muon showers were observed in the present experiment than in any experiment (previous work has been referred to by Porter and Stenerson 1969,

and very recent results have been given by Khrishnaswamy *et al.* 1970). The data consist of events observed over the depth range 1900–4000 hg cm^{-2} (the density of rock has been taken as $\rho = 2{\cdot}61$ g cm^{-3}—see Bergeson *et al.* 1967, 1968), and angular range 40–70°, and include the data presented in a preliminary report by Coats *et al.* (1970) to which the appropriate correction ($\sim 20\%$) has been made to the main detector data for the complex events that had to be hand-scanned. However, most of the pairs separated by more than 10 m, which are important in studying the tail of the transverse momentum distribution, comprise only about 3% of the total data. As this 3% is distributed over all depth and zenith angle ranges accepted, some consolidation is necessary. The approach adopted is to use the more abundant data at separations less than 10 m to deduce empirical rules for the depth and angular dependence of the decoherence curves, and to combine all the data from both the outriggers and the main detectors into a single decoherence curve using these rules.

Consequently the main detector data were assembled into 10° zenith angle bins and 500 hg cm^{-2} depth bins. Typical curves are shown in figure 3 for various depths in the zenith range 40–70°. Some obvious irregularities were being introduced into the decoherence curves by the distribution of depths over a 500 hg cm^{-2} depth bin, so as a first approximation the rates were corrected empirically to the depth at the centre of a 500 hg cm^{-2} bin. The best fits of the function $R_x = R_0 \exp(-X/X_0)$ were obtained by the method of least squares, and these are shown in figure 3 together with the corresponding values of X_0. In principle the experimental results can be used to determine the dependence of both X_0 and R_0 on muon threshold energy (E_μ) and zenith angle (θ). In practice the errors on the values of X_0 derived from the data are too large to establish the former, so the theoretical prediction of II has been adopted, namely,

$$\frac{X_0(E_\mu, \theta)}{X_0(1050, 45)} = \left(\frac{\sec\theta}{\sec 45}\right)^{1{\cdot}3} \left(\frac{1050}{E_\mu}\right)^{0{\cdot}8}. \tag{1}$$

Comparison of the absolute intensities of decoherence curves derived from the total data gives rise to the empirical intensity scaling

$$\frac{R_0(E_\mu, \theta)}{R_0(1050, 45)} = \left(\frac{1050}{E_\mu}\right)^{1{\cdot}95} \left(\frac{\sec 45}{\sec\theta}\right)^{1{\cdot}2}. \tag{2}$$

The above equations are used in the following way. Suppose a decoherence curve is measured at θ and h, corresponding to E_μ (the value of E_μ is given by the energy-loss equation $-\mathrm{d}E_\mu/\mathrm{d}h = a + bE_\mu$, with $a = 2{\cdot}5$ MeV g^{-1}cm^2, $b = 4{\cdot}0 \times 10^{-6}$ g^{-1}cm^2; fluctuations in muon energy loss are ignored at this stage). Then to convert to a decoherence curve at the datum (2500 hg cm^{-2} $\equiv$ 1050 GeV; $\theta = 45°$), $R_x(E_\mu, \theta)$ corresponding to $X(E_\mu, \theta)$ is converted to $R_x(1050, 45°)$ using equation (2), and plotted at $X(1050, 45°)$ derived from equation (1).

Comparing with II it will be noticed that the value of the exponent of E_μ in equation (2) differs from the value of 1·69 derived in II. This is due to the effect of fluctuations in energy loss. The value of 1·2 as the exponent of sec θ was determined empirically, and is somewhat larger than the value of 0·8 derived in II. However, the difference is not regarded as significant, in view of the positive correlation of depth with zenith angle owing to the nature of the terrain above the detector limiting the range of zenith angles obtainable at a given depth, and so limiting the accuracy to which the exponent can be determined.

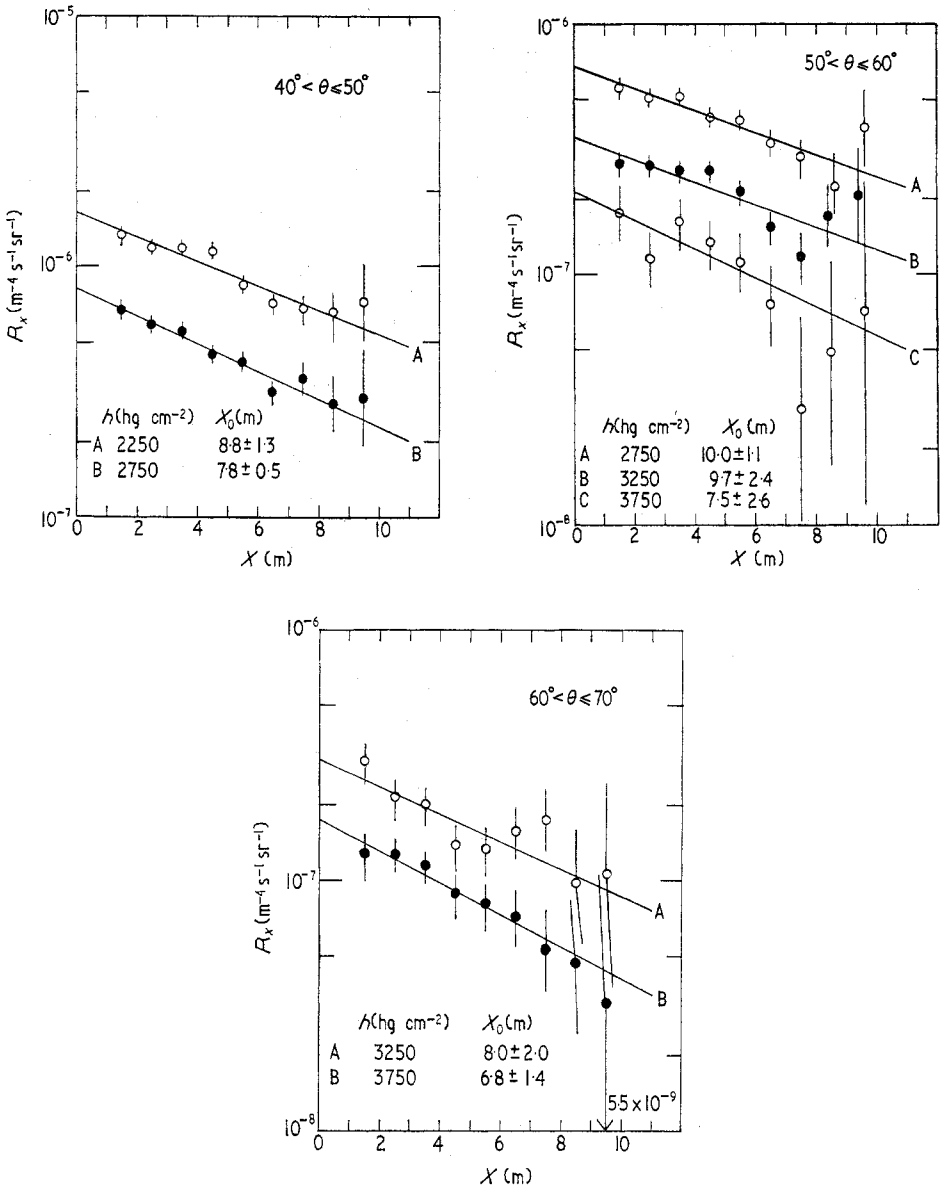

Figure 3. Measured rates in the main detector as a function of pair separation in metres for 500 hg cm^{-2} depth bins in the zenith angle ranges (*a*) 40–50°, (*b*) 50–60°, (*c*) 60–70°. Shown are the best fits to an exponential rate curve $\sim \exp(-X/X_0)$, the central values of the depth bins and the corresponding values of X_0.

The total data combined into a single decoherence curve at 2500 hg cm^{-2} and 45° are shown in figure 4. The error flags are statistical, but are based on the number of events contributing to pairs with a given separation rather than on the number of pairs, in order to take account of larger multiplicity events which can contribute more than one pair.

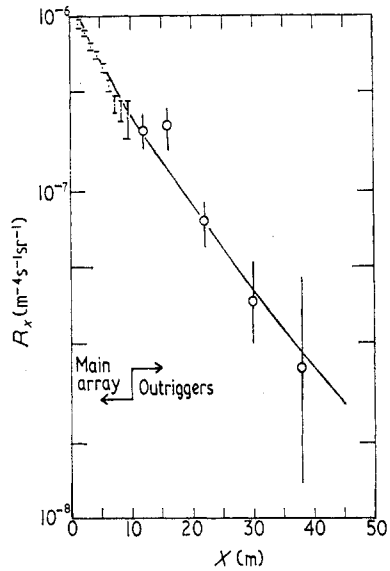

Figure 4. Measured decoherence curve scaled to 2500 hg cm^{-2} and 45°. The full line is the theoretical prediction from II using the transverse momentum distribution of Cocconi *et al.* (1961) for $\langle p_t \rangle = 0{\cdot}71$ GeV/c.

4. Discussion

A comparison between the measured decoherence curve and the curve derived in II on the basis of the transverse momentum distribution of Cocconi *et al.* (1961) and using the conservative interaction model, is made in figure 4. The theoretical curve has been normalized to the data by a factor 1·5, and the best fit to the data determined on the basis of minimum χ^2 gives a mean transverse momentum $\langle p_t \rangle = 0{\cdot}71 \pm 0{\cdot}09$ GeV/c. In the present paper the emphasis is on the shape of the decoherence curve rather than its absolute magnitude, and so a discussion of the difference in absolute intensities will be left to a later paper dealing with showers of various multiplicities in the main detector.

In order to test for internal consistency, the main detector data and the outrigger data were treated separately. The best value obtained for the former was $\langle p_t \rangle = 0{\cdot}68 \pm \frac{0{\cdot}08}{0{\cdot}05}$ GeV/c. The outrigger data was now subdivided into two depth ranges, 1900 to 2900 hg cm^{-2} and 2900 to 3900 hg cm^{-2}, and scaled to the datum (2500 hg cm^{-2} and 45°). Using the best fit to the main detector, the values of χ^2 obtained from the outrigger data alone were determined as a function of a factor N which multiplied the outrigger data. For the smaller depth range the minimum value of χ^2 occured at $N = 1{\cdot}0$, but for the larger depth range the minimum χ^2 was for $N = 1{\cdot}4$, indicating the possibility of internal inconsistency although it is quite possible that the effect is statistical in nature, for there are only 28 events in the larger depth range, compared with 78 in the range 1900–2900 hg cm^{-2}. Even if the inconsistency is real, however, its effect is relatively small—normalizing the larger depth outrigger data by the factor 1·4 results in $\langle p_t \rangle = 0{\cdot}68$ GeV/c, as compared with 0·71 GeV/c above—and so the value $N = 1{\cdot}0$ has been adopted for the total data.

A complete discussion of the conservative interaction model, together with predicted decoherence curves using different transverse momentum distributions is contained in II. The relevance of the X- process of Bergeson *et al.* (1967, 1968) is also discussed.

Acknowledgments

We would like to thank Professor A. W. Wolfendale for his encouragement and for many helpful discussions. We are also indebted to Adcock, Wdowczyk and Wolfendale for sharing pre-publication results of their shower development calculations with us.

Special thanks go to W. J. West, Jr., for carrying out the majority of the constructional work on the outriggers, and to T. M. Cannon, K. H. Davis and R. B. Ingebretsen for their contributions to computer analysis.

References

Adcock, C., Coats, R. B., Wolfendale, A. W., and Wdowczyk, J., 1970, *J. Phys.* A: *Gen. Phys.*, **3**, 697–707.

Bergeson, H. E., *et al.*, 1967, *Phys. Rev. Lett.*, **19**, 1487–91.

—— 1968, *Phys. Rev. Lett.*, **21**, 1089–93.

Coats, R. B., *et al.*, 1970, 11*th Int. Conf. on Cosmic Rays, Budapest*, to be published in *Acta Phys. Acad. Sci. Hung.*

Cocconi, G., Koester, L. G., and Perkins, D. H., 1961, *Lawrence Radiation Lab., High-Energy Phys. Study Seminars*, 28 part 2 UCID-1444, 1–36.

Hilton, L. K., Morris, M. L., and Stenerson, R. O., 1967, *Nucl. Instrum. Meth.*, **51**, 43–6.

Keuffel, J. W., and Parker, J. H., 1967, *Nucl. Instrum. Meth.*, **51**, 29–42.

Keuffel, J. W., *et al.*, 1970, 11*th Int. Conf. on Cosmic Rays, Budapest*, to be published in *Acta Phys. Acad. Sci. Hung.*

Khrishnaswamy, M. R., Menon, M. G. K., and Narasimhan, V. S., 1970, 11*th Int. Conf. on Cosmic Rays, Budapest*, to be published in *Acta Phys. Acad. Sci. Hung.*

Porter, L. G., and Stenerson, R. O., 1969, *J. Phys.* A: *Gen. Phys.*, **2**, 374–91.